ACS APPLIED POLYMER MATERIALS

Article

Cite This: *ACS Appl. Polym. Mater.* 2020, 2, 751−757

pubs.acs.org/acsapm

# Controlled Supramolecular Complexation of Cyclodextrin-Functionalized Polymeric Ionic Liquid Brushes

Serkan Demirci,*[†,‡] Selin Kinali-Demirci,[†,‡] and Brett VanVeller*[†]

[†]Department of Chemistry, Iowa State University, Ames, Iowa 50011 United States
[‡]Department of Chemistry, Amasya University, Amasya 05100 Turkey

*Supporting Information*

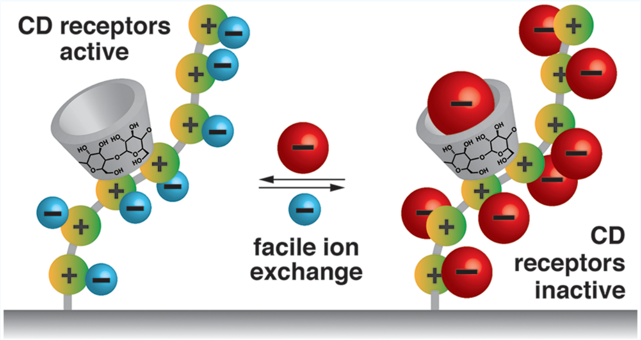

**ABSTRACT:** The control of molecular interactions between host and guest is of considerable importance for adsorption and release applications. To address this challenge, polymeric ionic liquid (PIL) brushes were prepared via reversible addition−fragmentation chain transfer polymerization, where we demonstrate that PILs confer a resistance to fouling of the material based on the counterion tunability of PILs. The anion-exchange of poly(1-vinyl-3-buthylimidazolium bromide) was used for the control of the host−guest interactions. Measurement of film thickness, contact angle, and surface morphology of the resulting surfaces were used to confirm the structural characteristics of the cyclodextrin-functionalized PIL brushes. The PIL brushes with switchable properties protect the immobilized host molecule against undesirable interactions without any morphological changes during storage and has potential application in bioseparation and biosensors.

**KEYWORDS:** *cyclodextrin, polymer brushes, polymeric ionic liquids, complexation, surface polymerization*

## INTRODUCTION

Functional polymer films possess several unique properties that can be modified to control their chemical and physical properties. The tunability of functional polymer films therefore provides unique opportunities to develop new materials for filtration, separation, biotechnology, biomaterials, and electronics.[1−5] For these applications, a variety of host molecules such as crown ether, cucurbituril, and cyclodextrin (CD) on the polymer brushes can provide multiple interactions with guest molecules.[6−12] Modification of polymer brushes with host molecules has offered polymer/material chemists opportunities to prepare smart surfaces that respond to different stimuli or changes in the environment via supramolecular interaction. Several supramolecular systems such as hydrogen bonding and inclusion complexes, among others, have frequently been used for the formation of complex macromolecular architectures.[13,14] In particular, CDs can form inclusion complexes with a variety of molecules due to the toroid-shaped molecular structure with a relatively hydrophobic interior cavity.[15,16] Thus, supramolecular systems have utilized CDs in many applications ranging from agriculture to biotechnology.[17−22] For example, CD-functionalized materials can provide a mechanism for separation and purification that can be used for the removal of organic molecules from liquid media and vapor phase.[23−26] Unfortunately, CD molecules can also be easily fouled by contaminants in these applications.

There is sustained interest in the preparation of CD-functionalized polymer brushes.[11,12,27−29] Strategies to protect CD-materials against fouling and undesirable interactions, however, are very limited in the literature. In our previous work, pH- and temperature-responsive cross-linked-polymer brushes were prepared by reversible addition−fragmentation chain transfer (RAFT) polymerization. The switchable capture and release capabilities of the stimuli-responsive brush-gels were also investigated by analyzing the host−guest interaction between methylene blue and CD under different environmental conditions.[30] In this work, we adopt a different approach to address the challenge of control of molecular interactions between host and guest molecules by using polymeric ionic liquids (PILs) brushes. In recent years, PILs have received increasing interest as a novel subclass of cationic polymers with unique physicochemical properties.[31−34] PILs incorporate the structural characteristics of ionic liquids (ILs) into polymer chains, which can lead to interesting and versatile polymeric materials for multiple applications.[35,36] More importantly, the characteristics of PILs can be tailored through simple exchange of anionic counterions,.[37] Our strategy exploits the stability and tunability of PIL brushes without sacrificing surface functionality or morphological changes. Moreover, the PILs brush system protects the $\beta$-cyclodextrin ($\beta$-CD) molecules against undesirable interactions during long-term storage.

**Received:** November 8, 2019
**Accepted:** December 10, 2019
**Published:** December 10, 2019

DOI: 10.1021/acsapm.9b01058

Scheme 1. Preparation and Controlled Supramolecular Complexation of β-CD Functionalized Polymer Brushes[a]

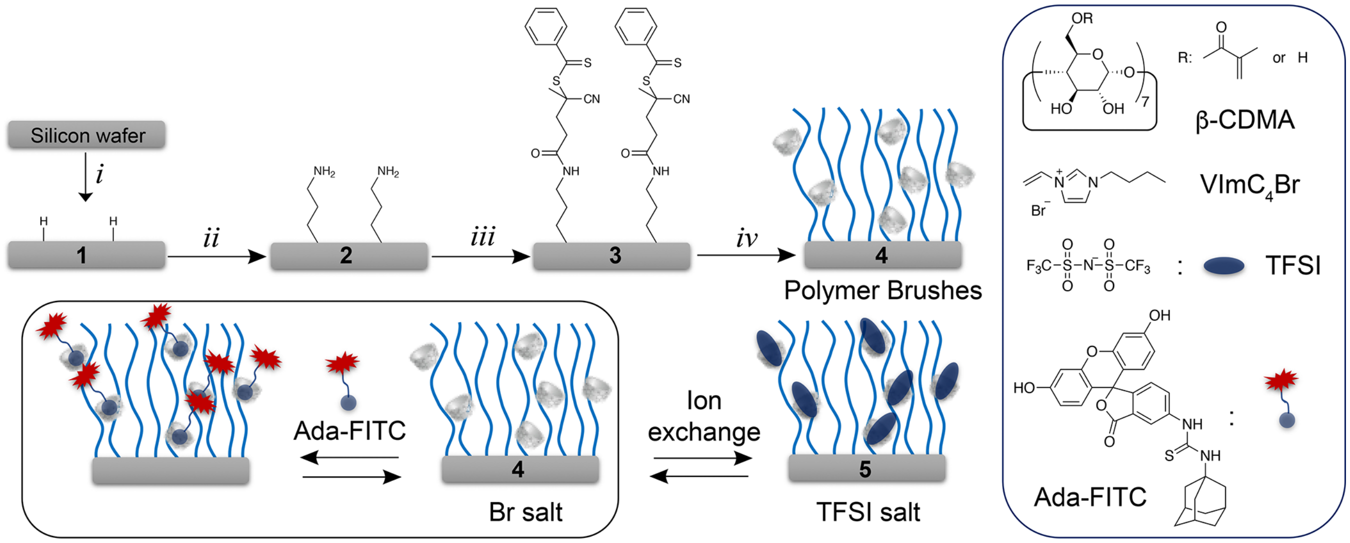

[a] *i*. Piranha solution, 2% HF; *ii*. *t*-BOC allylamine - UV, 25% TFA, 10% $NH_4OH$; *iii*. CPDBE, DCM, 60 h, rt; *iv*. $VImC_4Br$, β-CDMA, 24 h, 70 °C, Monomer/RAFT agent/Initiator:420/2/1. Chemical structure of monomers, TFSI and Ada-FITC.

## EXPERIMENTAL SECTION

**Materials.** All chemicals were analytical reagent grade and obtained from Sigma-Aldrich and used as purchased unless otherwise specified. Silicon (100) wafers (single side polished, N-type) were purchased from Aldrich. 1-Vinyl-3-buthylimidazolium bromide ($VImC_4Br$),[38] β-cyclodextrin methacrylate (β-CDMA),[39] and fluorescein isothiocyanate (FITC) labeled Ada (Ada-FITC)[40] were prepared according to the previously published protocols. Deionized water 18.2 MΩ.cm) was obtained from a Milli-Q water purification system (Millipore, Bedford, MA, U.S.A.).

**Surface-Initiated Polymerization.** Preparation of surface **3** was described in our previous works.[41−43] The poly($VImC_4Br$-*co*-β-CDMA) brushes were synthesized via RAFT polymerization. Surface **3** was placed in a glass reactor with monomer, β-CDMA (1% of monomer), 4-cyano-4-(phenylcarbonothioylthio)pentanoic acid as RAFT agent, 4,4′-azobis(4-cyanovaleric acid) as initiator (Monomer/RAFT agent/Initiator:420/2/1), and water/ethanol (10 mL). The mixture was degassed by three freeze−pump−thaw cycles and heated to 70 °C for 24 h. After the reaction was quenched in an ice bath, the surface **4** washed with water/ethanol mixture and dried under a stream of nitrogen. Poly($VImC_4TFSI$-*co*-β-CDMA) brushes were prepared via anion exchange reaction. Surface **4** was immersed in bis(trifluoromethane)sulfonimide lithium salt (LiTFSI) solution in water at room temperature for 24 h and then washed with water and ethanol and dried under a stream of nitrogen.

**Preparation of the Inclusion Complex.** Poly($VImC_4TFSI$)/β-CD inclusion complex was synthesized according to the freeze-drying method. First, 0.23 g of poly($VImC_4TFSI$) ($M_{n,\mathrm{SEC}} = 1.14 \times 10^4$ g mol$^{-1}$, DP = 26) was added to 5 mL of aqueous solution of β-CD (0.59 g) at 1:1 ratio (TFSI:β-CD). The solution was stirred for 24 h at room temperature. Finally, poly($VImC_4TFSI$)/β-CD inclusion complex powder was obtained after the solution was lyophilized for 48 h.

**Controlled Supramolecular Complexation between Target Molecule and β-CD-Functionalized PIL Brushes.** The fluorescein isothiocyanate isomer I (FITC) labeled 1-adamantylamine (Ada-FITC) molecule was used as a target molecule for the determination of controlled supramolecular complexation of cyclodextrin-functionalized polymeric ionic liquid brushes. The poly($VImC_4Br$-*co*-β-CDMA) brushes were immersed in an aqueous solution (25.0 μM) of Ada-FITC at room temperature for 24 h in the dark. After the brushes were rinsed five times with deionized water, the fluorescence images of the surfaces were recorded via Fluorescence microscope. Then poly($VImC_4Br$-*co*-β-CDMA) brushes were washed with deionized water at 40 °C for 10 min. For preparation of poly($VImC_4TFSI$-*co*-β-CDMA) brushes, the washed poly($VImC_4Br$-*co*-β-CDMA) brushes were immersed in LiTFSI solution in water at room temperature for 24 h and then washed with water and dried under a stream of nitrogen. Afterward, the poly($VImC_4TFSI$-*co*-β-CDMA) brushes were placed in an aqueous solution (25.0 μM) of Ada-FITC at room temperature for 24 h in dark, and fluorescence images were captured. Fluorescence intensities were calculated from fluorescence images via ImageJ software.

## RESULTS AND DISCUSSION

**Surface Modification and Characterization.** The PIL brushes were synthesized via RAFT polymerization (Scheme 1). The silicon wafers were cleaned by HF solution (1). HF treatment creates a uniform layer of Si−H groups across the surface (**1**). These uniformly distributed grafting points increase the grafting density of polymer chains. Surface **1** was then modified with allylamine using UV irradiation (**2**). The RAFT agent was immobilized on surface **2** through an amide coupling reaction (**3**), and the polymer brushes were subsequently synthesized via RAFT polymerization (**4**).

The progress of surface polymerization was confirmed using XPS spectra. The initial surface that displayed the RAFT agent (surface **3**) was confirmed by the presence of C 1s, O 1s, N 1s, S 2p, Si 2s, and Si 2p as previously reported.[30,41] After RAFT polymerization, the grafting of the PILs was confirmed by the presence of Br 3d (71.2 eV, Figure 1a), and the sharp increase in the N 1s signal at 402.3 eV, which is attributable to a positively charged nitrogen ($N^+$, Figure 1c).[44] Following treatment with LiTFSI, the disappearance of Br and appearance F (F 1s, 688.7 eV, Figure 1b), and $N^-$ (N 1s, 399.4 eV, Figure 1d) peaks confirmed the occurrence of the counteranion exchange reaction. We note that the $N^+/N^-$ ratio was calculated as 1.6, which is below the theoretical prediction of 2.0 based on the atomic composition of poly($VImC_4TFSI$-*co*-β-CDMA). The ratio of 1.6 indicates that there was more TFSI present than anticipated, and we surmise that this was due to complex formation between TFSI and β-CD which has been characterized previously.[45−47] This complex is critical to

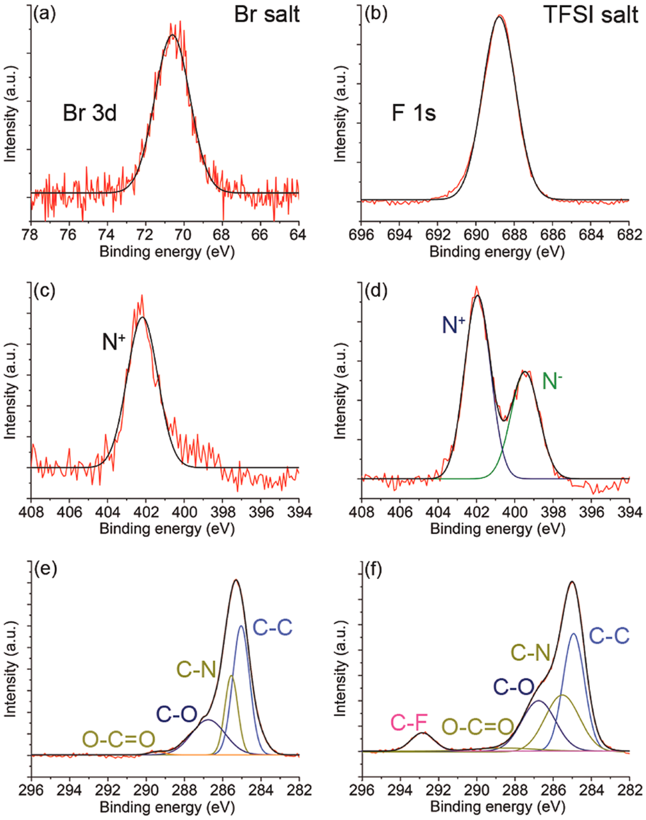

**Figure 1.** High-resolution XPS spectra of surface **4** (a, c, and e) and **5** (b, d, and f).

the antifouling and storage characteristics of the films that are described below.

A high-resolution C 1s scan was performed to obtain more detailed information about the chemical state of the PIL brush surface. Figure 1e,f shows C 1s spectra of poly(VImC$_4$Br-*co*-$\beta$-CDMA) (surface **4**) and poly(VImC$_4$TFSI-*co*-$\beta$-CDMA) (surface **5**) with their subpeaks. For poly(VImC$_4$Br-*co*-$\beta$-CDMA), the C 1s spectrum is deconvoluted into four subpeaks assigned to C−C at 285.0 eV, C−N at 285.6 eV, C−O at 286.8 eV, and O−C═O at 289.3 eV. The facile anion exchange was confirmed by the fitting of five components of the C 1s core-level peak having binding energy at 285.0, 285.4, 286.7, 288.9, and 292.8 eV attributed to C−C, C−N, C−O, O−C═O, and C−F, respectively. Chemical composition of the PILs surface was calculated from high-resolution C 1s spectra. C−O and O−C═O peaks originated from $\beta$-CD and used for the determination of methacrylate ratio. The peak ratio (C−O/O−C═O) that belongs to poly(VImC$_4$Br-*co*-$\beta$-CDMA) brushes was calculated as 18.9, which means that each $\beta$-CD molecule contained approximately two methacrylate units. On the other hand, the grafting density of $\beta$-CD was also determined as 5 and 5.9% for poly(VImC$_4$Br-*co*-$\beta$-CDMA) and poly(VImC$_4$TFSI-*co*-$\beta$-CDMA) brushes, respectively. These results were relatively higher than the feed ratio (1%) of the $\beta$-CD. This increase is caused by the $\beta$-CD which is randomly inserted and multiplied on the top of chains of PILs.

The counteranion exchange reaction and TFSI/$\beta$-CD complexation were also investigated by $^{19}$F NMR and FTIR spectroscopy (see Supporting Information for further discussion of FTIR results). While the complex between monomeric $\beta$-CD and TFSI partners has been characterized previously,[45−47] we sought to confirm that this association was still operative with PIL. $^{19}$F NMR spectrum analysis of linear polymers in solution was carried out (Figure 2) to probe the supramolecular complexation of $\beta$-CD and poly(VImC$_4$TFSI). No $^{19}$F NMR signal was observed for the poly(VImC$_4$Br) species. Following treatment with LiTFSI, an $^{19}$F NMR signal appeared at −77.91 ppm to indicate formation of poly(VImC$_4$TFSI). When $\beta$-CD was added (molar ratio of TFSI:$\beta$-CD, 1:1), a characteristic shift[45−47] in the $^{19}$F NMR signal of the TFSI to higher frequency (−77.86 ppm) indicated the supramolecular interaction between $\beta$-CD and TFSI. Following another anion exchange reaction, the fluorine signal disappeared completely. These results confirmed that the TFSI group was encapsulated within the cavity of $\beta$-CD through host−guest interaction.

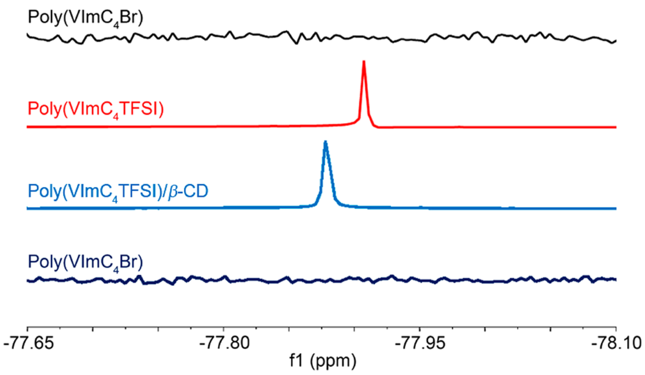

**Figure 2.** $^{19}$F NMR spectra of poly(VImC$_4$Br), poly(VImC$_4$TFSI), and poly(VImC$_4$TFSI)/$\beta$-CD complex (TFSI:$\beta$-CD molar ratio is 1:1) in DMSO.

The polymer brush synthesis and ion exchange were also tracked via static water contact angle measurement (Figure 3). The static water contact angle of surface **3**, functionalized with 4-cyano-4-(phenylcarbonothioylthio)pentanoic acid, was 63 ± 2° which was higher than the value of 55 ± 3° for the surface **2** before the immobilization. These values are consistent with the literature and indicate the attachment of the more hydrophobic RAFT agent.[48] When the PIL brushes were prepared, the static water contact angle of the surface decreased substantially to about 45 ± 4°, consistent with the hydrophilic nature of poly(VImC$_4$Br-*co*-$\beta$-CDMA). After the anion-exchange reaction, a significant change in surface wettability was characterized by a dramatic increase in the static water contact-angle from 45 ± 5° (poly(VImC$_4$Br-*co*-$\beta$-CDMA)) to 102 ± 3° (poly(VImC$_4$TFSI-*co*-$\beta$-CDMA)) (Figure 3). As alluded to earlier, the chemical structure of the cation and the anion both play a vital role in controlling the characteristics and properties of the PILs. Recent studies showed that performing anion exchanges on PILs greatly influenced the solubility of the polymers.[36,37,49] The solubility characteristics of the PIL brushes were tuned by anion exchange in the presence of excesses of salts producing polymers that ranged from hydrophilic to hydrophobic. The hydrophilic poly(VImC$_4$Br-*co*-$\beta$-CDMA) layer adopts an extended chain conformation to allow complexation between host and guest molecules, while the hydrophobic poly(VImC$_4$TFSI-*co*-$\beta$-CDMA) layer protects the guest molecules with TSFI counterion.

To further characterize the PIL brushes on the silicon surface, the surface morphology was investigated by AFM, and

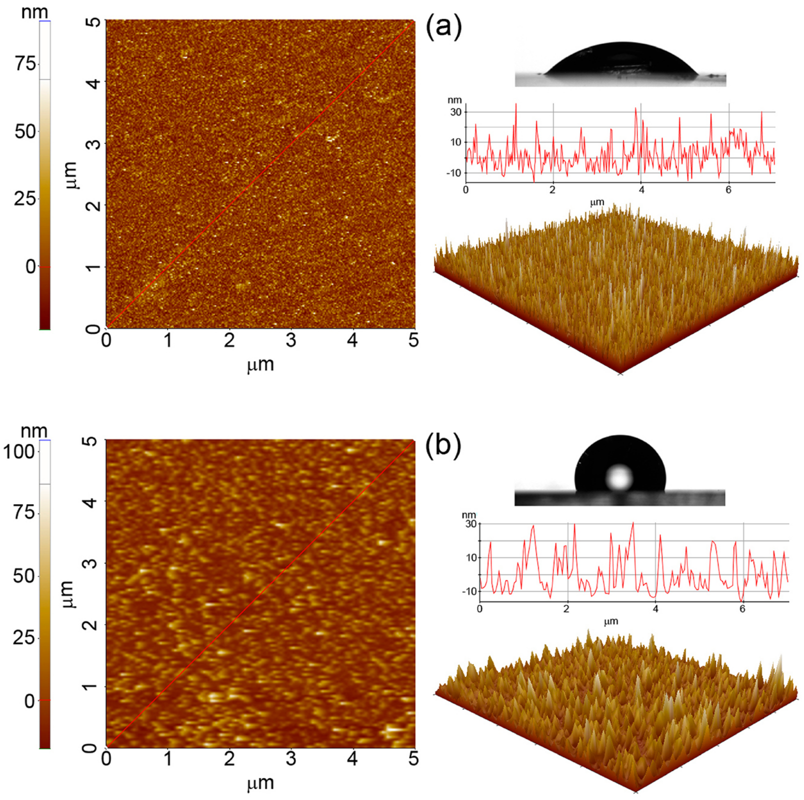

**Figure 3.** AFM images, cross-sectional analysis, and photographs in ambient conditions of 5.0 μL water droplets for Br salt (a) and TFSI salt (b) of polymer brushes.

the corresponding images are shown in Figure 3. It was noticed that the surface morphology was altered after coating with poly(VImC$_4$Br-*co*-β-CDMA), compared with the Si-RAFT surfaces. Root-mean-square (RMS) roughness for Si-RAFT was changed from 0.80 nm[48] to 6.6 nm upon subsequent grafting of poly(VImC$_4$Br-*co*-β-CDMA) chains. The increase in RMS roughness values of the polymer brushes was possibly due to uneven distribution of collapsed poly(VImC$_4$Br-*co*-β-CDMA) graft chains on the surface. Overall, the film morphology appeared as needle-like structure, and the ellipsometric film thicknesses of the poly(VImC$_4$Br-*co*-β-CDMA) brushes were measured to be 34 ± 4 nm. The effect of counteranions on the surface morphology of the polymer brush was investigated by characterizing and comparing the surface morphologies of PIL brushes from Br and TFSI salts. The poly(VImC$_4$TFSI-*co*-β-CDMA) brushes were fabricated via anion exchange reaction. For this, poly(VImC$_4$Br-*co*-β-CDMA) brushes were immersed in the LiTFSI solution, then washed with deionized-water, acetone and THF in order. As shown in Figure 3b, no significant differences were observed between the morphology of poly(VImC$_4$Br-*co*-β-CDMA) and poly(VImC$_4$TFSI-*co*-β-CDMA) brushes. In the cases of TFSI salts, the surface roughness (8.6 nm) and ellipsometric thickness (42 ± 5 nm) of the brushes were slightly increased because of the steric hindrance of TFSI group.

**Controlled Supramolecular Complexation.** As mentioned previously, CD can participate in host/guest complexes by inclusion of suitable molecules from liquid media and the vapor phase. However, this ability of CD molecules can cause problems during the periods of storage. The protection ability of the PIL chains against undesirable interaction was also tested using a model organic compound: The adamantyl-FITC conjugate (Ada-FITC) was chosen as a model molecule for the controlled supramolecular complexation with CD. Controlled supramolecular complexation of β-CD-functionalized brushes is illustrated in Scheme 1. The influence of counteranion on complexation of β-CD with Ada-FITC was monitored by UV–vis spectrophotometry at 492 nm and fluorescence microscopy.

Figure 4 shows the Ada-FITC removal (%) from the solution with contact time for the adsorption of Ada-FITC onto PILs brushes under environmental conditions. The adsorption of Ada-FITC onto the poly(VImC$_4$Br-*co*-β-CDMA) brushes increased with increased time. The poly(VImC$_4$Br-*co*-β-CDMA) brushes is hydrophilic and allowed the Ada-FITC adsorption by β-CD molecules at room temperature. On the other hand, the adsorption of Ada-FITC was unfavorable for poly(VImC$_4$TFSI-*co*-β-CDMA)

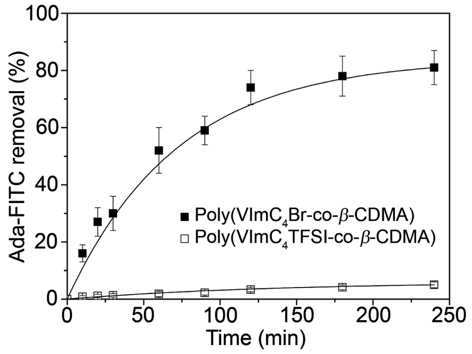

**Figure 4.** Variation of Ada-FITC removal with contact time for the adsorption of Ada-FITC onto PILs brushes under the environmental condition.

brushes. We propose that the dramatically reduced absorption of Ada-FITC arises because of the blocking of *β*-CD cavities with TFSI ions to prevent Ada-FITC adsorption. Indeed, the affinity of *β*-CD for TFSI is actually higher than for adamantyl derivatives.[44,45] It can be observed from Figure 4 that after 240 min of adsorption, the removal efficiencies of poly(VImC$_4$Br-*co*-*β*-CDMA) and poly(VImC$_4$TFSI-*co*-*β*-CDMA) were 81 ± 6%, and 5 ± 1%, respectively.

From a practical point of view, stability, and reusability are essential features for adsorption applications. In this study, the reusability of the PILs brushes was investigated in a cyclic manner by measuring the fluorescence intensity of PILs brush surfaces and adsorption of Ada-FITC through Br and TFSI salt cycles (Figure 5). The Ada-FITC desorbed after sonication cleaning at 40 °C, then anion was exchanged. The anion exchange procedure was repeated five times. The poly(VImC$_4$Br-*co*-*β*-CDMA) brushes showed a subtle decrease in performance toward the removal of Ada-FITC over time. This observation could be explained by the decreased exchanging efficiency with increasing repeated cycles. Overall, these results suggest that PIL brushes are a reusable platform.

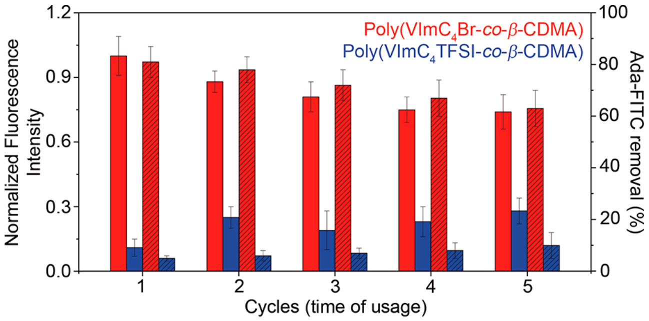

**Figure 5.** Normalized fluorescence intensity of PILs brushes and removal efficiency (%) of Ada-FITC (patterned) in repeated cycles.

To further test the up-take ability of the PIL surfaces, we compared the performance of PILs brushes against different ratios of Ada-FITC and the competitive guest molecule 1-adamantanecarboxylic acid (Ada-COOH) (Figure 6a). Using fluorescence microscopy, we were able to confirm that the fluorescence intensity of Ada-FITC was higher in poly(VImC$_4$Br-*co*-*β*-CDMA) films than for poly(VImC$_4$TFSI-*co*-*β*-CDMA) films which was consistent with the "up-take" experiments in Figure 4. As the amount of Ada-COOH was increased within the molar ratio, we observed a consistent decrease in fluorescence intensity from the poly(VImC$_4$Br-*co*-*β*-CDMA). These results indicate that Ada-COOH effectively competes with Ada-FITC for the *β*-CD sites within the film, which allowed us to exam the films antifouling potential.

The antifouling behavior of the PILs brushes was tested using Ada-COOH as the fouling source. Poly(VImC$_4$Br-*co*-*β*-CDMA) and poly(VImC$_4$TFSI-*co*-*β*-CDMA) films were immersed in an aqueous solution of Ada-COOH for the exposure times indicated (Figure 6b). After exposure, the poly(VImC$_4$Br-*co*-*β*-CDMA) brushes were washed with deionized water and then immersed in a solution of Ada-FITC. The depletion of Ada-FITC from the solution was then determined by UV−vis spectrophotometry at 492 nm. The ability of the poly(VImC$_4$Br-*co*-*β*-CDMA) brushes to scavenge Ada-FITC from solution was significantly compromised (Figure 6b (red)) because Ada-COOH served to bind and foul the *unprotected β*-CD moieties in the film. This same procedure was then repeated with poly(VImC$_4$TFSI-*co*-*β*-CDMA) brushes with the important caveat that poly(VImC$_4$TFSI-*co*-*β*-CDMA) films were converted to poly(VImC$_4$Br-*co*-*β*-CDMA) films through ion exchange prior to treatment with Ada-FITC (Figure 6b (blue)). The TFSI counterions in the poly(VImC$_4$TFSI-*co*-*β*-CDMA) brush served to *protect* the *β*-CD moieties such that ion exchange leads to a functional polymer brush that was able to effectively scavenge Ada-FITC from solution. These results clearly demonstrate the potential of poly(VImC$_4$TFSI-*co*-*β*-CDMA) brushes to guard against the fouling of surface functional groups during long-term storage.

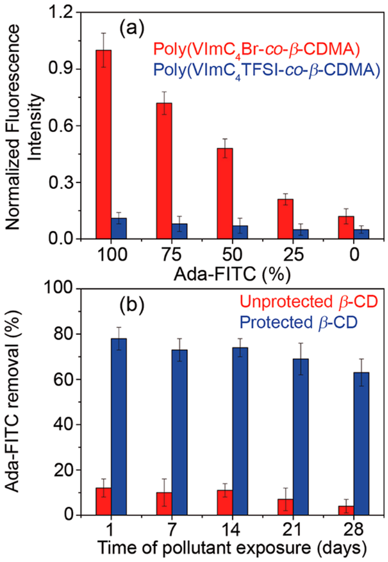

**Figure 6.** (a) Normalized fluorescence intensity of PILs brushes with different Ada-FITC (%) feed ratio. (b) Variation of Ada-FITC removal with exposure time.

## CONCLUSIONS

In conclusion, *β*-CD-functionalized PIL brushes with switchable properties were successfully prepared via RAFT polymerization to protect the *β*-CD against contamination. Using techniques such as XPS, ellipsometry, and AFM, we confirmed the structure of *β*-CD-functionalized PIL brushes during each stage of surface functionalization. Static water-contact-angle measurements showed that an anion exchange reaction could tune the wettability of the PIL brushes. After anion exchange, an inclusion complex between *β*-CD and the TFSI counterion prevents undesirable host−guest interactions during storage. The complexation behavior of the brushes could be controlled and switched by the identity of the counteranions. This new strategy for the preparation of responsive and contamination-free surfaces may provide opportunities to develop innovative responsive materials for various applications. Additionally, our newly developed *β*-CD-functionalized polymer brushes may be potentially useful for bioseparation, biosensor, and biomedical engineering via supramolecular interaction.

## ASSOCIATED CONTENT

### Ⓢ Supporting Information

The Supporting Information is available free of charge at https://pubs.acs.org/doi/10.1021/acsapm.9b01058.

Synthetic procedure and characterization of small molecules and polymers; UV−vis and IR characterization of surface (PDF)

## AUTHOR INFORMATION

### Corresponding Authors

*E-mail: srkndemirci@gmail.com.
*E-mail: bvv@iastate.edu.

### ORCID

Serkan Demirci: 0000-0002-4753-2069
Selin Kinali-Demirci: 0000-0001-5363-9412
Brett VanVeller: 0000-0002-3792-0308

### Notes

The authors declare no competing financial interest.

## ACKNOWLEDGMENTS

SD received financial support from TUBITAK-BIDEB 2219-International Postdoctoral Research Fellowship Programme for this study. BV would like to acknowledge the National Science Foundation (Grant 1848261) and donors of the American Chemical Society Petroleum Research Fund (57219DNI4).

## REFERENCES

(1) Giussi, J. M.; Cortez, M. L.; Marmisolle, W. A.; Azzaroni, O. Practical Use of Polymer Brushes in Sustainable Energy Applications: Interfacial Nanoarchitectonics for High-Efficiency Devices. *Chem. Soc. Rev.* **2019**, *48*, 814−849.

(2) Keating, J. J., IV; Imbrogno, J.; Belfort, G. Polymer Brushes for Membrane Seperations: A Review. *ACS Appl. Mater. Interfaces* **2016**, *8*, 28383−28399.

(3) Yu, Q.; Ista, L. K.; Gu, R.; Zauscher, S.; Lopez, G. P. Nanopatterned Polymer Brushes: Conformation, Fabrication and Applications. *Nanoscale* **2016**, *8*, 680−700.

(4) Das, S.; Banik, M.; Chen, G.; Sinha, S.; Mukherjee, R. Polyelectrolyte Brushes: Theory, Modelling, Synthesis and Applications. *Soft Matter* **2015**, *11*, 8550−8583.

(5) Zoppe, J. O.; Ataman, N. C.; Mocny, P.; Wang, J.; Moraes, J.; Klok, H.-A. Surface-Initiated Controlled Radical Polymerization: State-of-the-Art, Opportunities, and Challenges in Surface and Interface Engineering with Polymer Brushes. *Chem. Rev.* **2017**, *117*, 1105−1318.

(6) Jiang, H.; Xu, F.-J. Biomolecule-Functionalized Polymer Brushes. *Chem. Soc. Rev.* **2013**, *42*, 3394−3426.

(7) Schüwer, N.; Klok, H. A. A Potassium-Selective Quartz Crystal Microbalance Sensor Based on Crown-Ether Functionalized Polymer Brushes. *Adv. Mater.* **2010**, *22*, 3251−3255.

(8) Ahn, Y.; Jang, Y.; Selvapalam, N.; Yun, G.; Kim, K. Supramolecular Velcro for Reversible Underwater Adhesion. *Angew. Chem., Int. Ed.* **2013**, *52*, 3140−3144.

(9) Marten, G. U.; Gelbrich, T.; Ritter, H.; Schmidt, A. M. A Magnetoresponsive Drug Delivery System via $\beta$-Cyclodextrin Functionalized Magnetic Polymer Brushes. *IEEE Trans. Magn.* **2013**, *49*, 364−372.

(10) Panahi, H. A.; Alaei, H. S. $\beta$-Cyclodextrin/Thermosensitive Containing Polymer Brushes Grafted onto Magnetite Nano-Particles for Extraction and Determination of Venlafaxine in Biological and Pharmaceutical Samples. *Int. J. Pharm.* **2014**, *476*, 178−184.

(11) Deng, J.; Liu, X.; Shi, W.; Cheng, C.; He, C.; Zhao, C. Light-Triggered Switching of Reversible and Alterable Biofunctionality via $\beta$-Cyclodextrin/Azobenzene-Based Host-Guest Interaction. *ACS Macro Lett.* **2014**, *3*, 1130−1133.

(12) Zhang, Y.; Ren, L.; Tu, Q.; Wang, X.; Liu, R.; Li, L.; Wang, J. C.; Liu, W.; Xu, J.; Wang, J. Fabrication of Reversible Poly(dimethylsiloxane) Surfaces via Host-Guest Chemistry and Their Repeated Utilization in Cardiac Biomarker Analysis. *Anal. Chem.* **2011**, *83*, 9651−9659.

(13) Schmidt, B. V. K. J.; Hetzer, M.; Ritter, H.; Barner-Kowollik, C. Complex Macromolecular Architecture Design via Cyclodextrin Host/Guest Complexes. *Prog. Polym. Sci.* **2014**, *39*, 235−249.

(14) Chen, Y.; Klimczak, A.; Galoppini, E.; Lockard, J. V. Structural Interrogation of a Cucurbit[7]uril-Ferrocene Host-Guest Complex in the Solid State: A Raman Spectroscopy Study. *RSC Adv.* **2013**, *3*, 1354−1358.

(15) Szejtli, J. Introduction and General Overview of Cyclodextrin Chemistry. *Chem. Rev.* **1998**, *98*, 1743−1753.

(16) Hedges, A. R. Industrial Applications of Cyclodextrins. *Chem. Rev.* **1998**, *98*, 2035−2044.

(17) Shi, J.; Chen, Z.; Wang, B.; Wang, L.; Lu, T.; Zhang, Z. Reactive Oxygen Species-Manipulated Drug Release from a Smart Envelope-Type Mesoporous Titanium Nanovehicle for Tumor Sonodynamic-Chemotherapy. *ACS Appl. Mater. Interfaces* **2015**, *7*, 28554−28565.

(18) Ma, X.; Zhou, N.; Zhang, T.; Guo, Z.; Hu, W.; Zhu, C.; Ma, D.; Gu, N. In situ Formation of Multiple Stimuli-Responsive Poly-[(methyl vinyl ether)-alt-(maleic acid)]-Based Supramolecular Hydrogels by Inclusion Complexation Between Cyclodextrin and Azobenzene. *RSC Adv.* **2016**, *6*, 13129−13136.

(19) Del Valle, E. M. M. Cyclodextrins and Their Uses: A Review. *Process Biochem.* **2004**, *39*, 1033−1046.

(20) Wang, Y.-F.; Zhang, D.-L.; Zhou, T.; Zhang, H.-S.; Zhang, W.-Z.; Luo, L.; Zhang, A.-M.; Li, B.-J.; Zhang, S. A Reversible Functional Supramolecular Material Formed by Host-Guest Inclusion. *Polym. Chem.* **2014**, *5*, 2922−2927.

(21) Landy, D.; Mallard, I.; Ponchel, A.; Monflier, E.; Fourmentin, S. Remediation Technologies Using Cyclodextrins: An Overview. *Environ. Chem. Lett.* **2012**, *10*, 225−237.

(22) Zhao, R.; Wang, Y.; Li, X.; Sun, B.; Wang, C. Synthesis of $\beta$-Cyclodextrin-Based Electrospun Nanofiber Membranes for Highly Efficient Adsorption and Separation of Methylene Blue. *ACS Appl. Mater. Interfaces* **2015**, *7*, 26649−26657.

(23) Uyar, T.; Havelund, R.; Hacaloglu, J.; Besenbacher, F.; Kingshott, P. Functional Electrospun Polystyrene Nanofibers Incorporating $\alpha$-, $\beta$-, and $\gamma$- Cyclodextrins: Comparison of Molecular Filter Performance. *ACS Nano* **2010**, *4*, 5121−5130.

(24) Kayaci, F.; Uyar, T. Electrospun/Cycloextrin Nanofibers for Entrapment of Volatile Organic Compounds. *Polym. Eng. Sci.* **2014**, *54*, 2970−2978.

(25) Morin-Crini, N.; Crini, G. Environmental Applications of Water-Insoluble $\beta$-Cyclodextrin-Epichlorohydrin Polymers. *Prog. Polym. Sci.* **2013**, *38*, 344−368.

(26) Schofield, W. C. E.; Bain, C. D.; Badyal, J. P. S. Cyclodextrin-Functionalized Hierarchical Porous Architectures for High-Throughput Capture and Release of Organic Pollutants from Wastewater. *Chem. Mater.* **2012**, *24*, 1645−1653.

(27) Shi, X.; Chen, G.-J.; Wang, Y.; Yuan, L.; Zhang, Q.; Haddleton, D. M.; Chen, H. Control the Wettability of Poly(*N*-isopropylacrylamide-co-1-adamantan-1-ylmethyl acrylate) Modified Surfaces: The More Ada, the Bigger Impact? *Langmuir* **2013**, *29*, 14188−14195.

(28) Zengin, A.; Tamer, U.; Caykara, T. SERS Detection of Polyaromatic Hydrocarbons on a $\beta$-Cyclodextrin Containing Polymer Brush. *J. Raman Spectrosc.* **2018**, *49*, 452−461.

(29) Lamping, S.; Stricker, L.; Ravoo, B. J. Responsive Surface Adhesion Based on Host-Guest Interaction of Polymer Brushes with Cyclodextrins and Arylazopyrazoles. *Polym. Chem.* **2019**, *10*, 683−690.

(30) Demirci, S. Crosslinked-Polymer Brushes with Switchable Capture and Release Capabilities. *Polymers* **2018**, *10*, 956.

(31) Tröger-Müller, T.; Liedel, C. Sustainable Polyimidazolium Networks as Versatile Hydrogel Materials. *ACS Appl. Polym. Mater.* **2019**, *1*, 2606−2612.

(32) Devasurendra, A. M.; Zhang, C.; Young, J. A.; Tillekeratne, L. M. V.; Anderson, J. L.; Kirchhoff, J. R. Electropolymerized Pyrrole-Based Conductive Polymeric Ionic Liquids and Their Application for

Solid-Phase Microextraction. *ACS Appl. Mater. Interfaces* **2017**, *9*, 24955−24963.

(33) Korolovych, V. F.; Erwin, A.; Stryutsky, A.; Lee, H.; Heller, W. T.; Shevchenko, V. V.; Bulavin, L. A.; Tsukruk, V. V. Thermally Responsive Hyperbranched Poly(ionic liquid)s: Assembly and Phase Transformations. *Macromolecules* **2018**, *51*, 4923−4937.

(34) Grygiel, K.; Lee, J.-S.; Sakaushi, K.; Antonietti, M.; Yu-an, Y. Thiazolium Poly(ionic liquid)s: Synthesis and Application as Binder for Lithium-Ion Batteries. *ACS Macro Lett.* **2015**, *4*, 1312−1316.

(35) Gallastegui, A.; Porcarelli, L.; Palacios, R. E.; Gómez, M. L.; Mecerreyes, D. Catechol-Containing Acrylic Poly(ionic liquid) Hydrogels as Bioinspired Filters for Water Decontamination. *ACS Appl. Polym. Mater.* **2019**, *1*, 1887−1895.

(36) Mecerreyes, D. Polymeric Ionic Liquids: Broadening the Properties and Applications of Polyelectrolytes. *Prog. Polym. Sci.* **2011**, *36*, 1629−1648.

(37) Dong, Y.-S.; Xiong, X.-H.; Lu, X.-W.; Wu, Z.-Q.; Chen, H. Antibacterial Surfaces Based on Poly(cationic liquid) Brushes: Switchability Between Killing and Releasing via Anion Counterion Switching. *J. Mater. Chem. B* **2016**, *4*, 6111−6116.

(38) Zhang, J.; Xu, D.; Guo, J.; Sun, Z.; Qian, W.; Zhang, Y.; Yan, F. $CO_2$ Responsive Imidazolium-Type Poly(ionic liquid) Gels. *Macromol. Rapid Commun.* **2016**, *37*, 1194−1199.

(39) Kettel, M. J.; Schaefer, K.; Pich, A.; Moeller, M. Functional PMMA Nanogels by Cross-Linking with Cyclodextrin Methacrylate. *Polymer* **2016**, *86*, 176−188.

(40) Fang, G.; Xu, M.; Zeng, F.; Wu, S. $\beta$-Cyclodextrin as the Vehicle for Forming Ratiometric Mercury Ion Sensor Usable in Aqueous Media, Biological Fluids, and Live Cells. *Langmuir* **2010**, *26*, 17764−17771.

(41) Demirci, S.; Kinali-Demirci, S.; Jiang, S. A Switchable Polymer Brush System for Antifouling and Controlled Detection. *Chem. Commun.* **2017**, *53*, 3713−3716.

(42) Demirci, S.; Kinali-Demirci, S.; Caykara, T. Stimuli-Responsive Diblock Copolymer Brushes via Combination of "Click Chemistry" and Living Radical Polymerization. *J. Polym. Sci., Part A: Polym. Chem.* **2013**, *51*, 2677−2685.

(43) Demirci, S.; Kinali-Demirci, S.; Caykara, T. A New Selenium-Based RAFT Agent for Surface-Initiated RAFT Polymerization of 4-Vinylpyridine. *Polymer* **2013**, *54*, 5345−5350.

(44) Wu, J.; Zhang, D.; Zhang, L.; Wu, B.; Xiao, S.; Chen, F.; Fan, P.; Zhong, M.; Tan, J.; Chu, Y.; Yang, J. Long-Term Stability and Salt-Responsive Behavior of Polyzwitterionic Brushes with Cross-Linked Structure. *Prog. Org. Coat.* **2019**, *134*, 153−161.

(45) He, Y.; Chen, Q.; Xu, C.; Zhang, J.; Shen, X. Interaction Between Ionic Liquids and $\beta$-Cyclodextrin: A Discussion of Association Pattern. *J. Phys. Chem. B* **2009**, *113*, 231−238.

(46) Amajjahe, S.; Ritter, H. Anion Complexation of Vinylimidazolium Salts and Its Influence on Polymerization. *Macromolecules* **2008**, *41*, 716−718.

(47) Yuan, C.; Guo, J.; Tan, M.; Guo, M.; Qiu, L.; Yan, F. Multistimuli Responsive and Electroactive Supramolecular Gels Based on Ionic Liquid Gemini Guest. *ACS Macro Lett.* **2014**, *3*, 271−275.

(48) Demirci, S.; Caykara, T. RAFT-Mediated Synthesis of Cationic Poly[(ar-vinylbenzyl)trimethylammonium chloride] Brushes for Quantitative DNA Immobilization. *Mater. Sci. Eng., C* **2013**, *33*, 111−120.

(49) Yuan, J.; Antonietti, M. Poly(ionic liquid)s: Polymers Expanding Classical Property Profiles. *Polymer* **2011**, *52*, 1469−1482.